

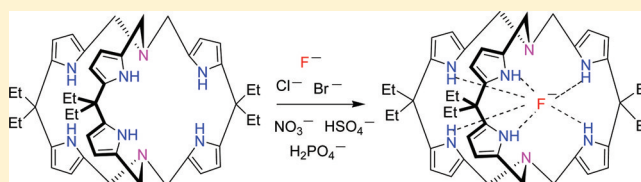
Dipyrrolylmethane-based Macrobicyclic Azacryptand: Synthesis, X-ray Structures, Conformational and Anion Binding Properties

Tapas Guchhait and Ganesan Mani*

Department of Chemistry, Indian Institute of Technology, Kharagpur, India 721 302

S Supporting Information

ABSTRACT: A new class of macrobicyclic azacryptand containing dipyrrolylmethane subunits with nitrogen bridgeheads was synthesized by the Mannich reaction of the dipyrrolylmethane in the presence of aqueous ammonia. The azacryptand exhibits a staggered conformation in the solid state, but is in a dynamic equilibrium with the eclipsed conformation in solution studied by the variable-temperature ^1H NMR methods. The azacryptand has a specific size suitable only for fluoride ion; large anions such as NO_3^- bind in the clefts of the macrobicyclic as shown by the X-ray structures of its fluoride ion inclusion and the nitrate anion complexes. The anion binding studies showed that it has high selectivity and affinity for fluoride ion in acetone over other anions studied, which was supported by ^1H and ^{19}F NMR methods. The azacryptand has fast fluoride ion-mediated proton–deuterium exchanges with acetone- d_6 studied by the ^{19}F NMR method.



INTRODUCTION

Since the first report of the chloride inclusion complex of Katapinands by Park and Simmons in 1968¹ and the independent pioneering work of Lehn and co-workers,² the anion recognition chemistry by synthetic receptor systems remains an active area of research in the supramolecular chemistry.³ Anions play important roles in biological and environmental systems. Given the nature of anions, developing a receptor that binds a specific anion with high selectivity and affinity is a challenging task.⁴ Although several cyclic and acyclic systems have been developed to study anion recognitions,⁵ macrobicyclic cryptand-like anion receptors have attracted a great attention owing to their unique three-dimensional cavities.⁶ Their exclusive selectivity and high affinity for a specific anion have been demonstrated; for an example, C2-bistren cryptand has very high affinity for fluoride ion in an aqueous solution.⁷ Besides, cryptands exhibit conformational properties that are interesting to study by NMR methods.⁸

To modulate the anion and ion-pair recognition capabilities of calixpyrrole type molecules, a variety of macrocyclic systems have been developed.⁹ On the contrary, only a few pyrrole-based macrobicyclic cryptand-like systems have been developed to date for anion recognition.¹⁰ However, there is a demand for developing better anion receptors with high selectivity and affinity for a specific anion for many applications.¹¹

As continuation of our interest to develop synthetic anion receptor systems containing pyrrole subunits through Mannich reactions,¹² here we first report the synthesis, structural characterization, conformational study by variable-temperature NMR methods, and anion binding properties of a new class of azacryptand **1** containing dipyrrolylmethane subunits with nitrogen bridgeheads, which acts as a selective neutral receptor for fluoride ion in a competitive solvent, acetone. In addition,

we report the X-ray structures of its fluoride ion inclusion and the nitrate anion complexes and the proton–deuterium exchanges by the ^{19}F NMR method.

RESULTS AND DISCUSSION

Synthesis of Azacryptand. In contrast to the cryptand-like calixpyrrole systems with bridgehead carbons,¹⁰ a new class of cryptand-like calixdipyrrolylmethane with bridgehead nitrogen atoms called azacryptand **1** was synthesized by the Mannich reaction of diethyldipyrrolylmethane with a mixture of aqueous ammonia and formaldehyde in a poor yield (3%), owing to the formation of several other products including new 1,9-bis-(ethoxymethyl)dipyrrolylmethane **2** formed in 3% yield (Scheme 1). **1** and **2** were separated by basic alumina column chromatography. The yield of **1** could not be improved by using NH_4Cl instead of ammonia even under dilute conditions. The azacryptand **1** can be viewed as a macrocycle called azacalix[2]dipyrrolylmethane^{12b} strapped with a dipyrrolylmethane moiety.

The ^1H NMR spectrum of **1** in CDCl_3 showed a broad singlet at δ 8.46 for the pyrrolic NH protons, indicating the presence of only one conformer with either the *in/in* or *out/out* orientation of the lone pairs of electrons in the bridgehead N atoms with respect to the cavity of the azacryptand **1**.^{8a} In addition, a very broad signal at δ 3.42 for the $-\text{NCH}_2-$ methylene protons was observed, indicating a torsional motion about the bridgehead N---N axis.

Conformational Study. To understand the torsional motion of **1** in solution, the variable-temperature ^1H NMR studies were carried out and the spectra are given in Figure 1. On the other hand,

Received: September 23, 2011

Published: November 8, 2011

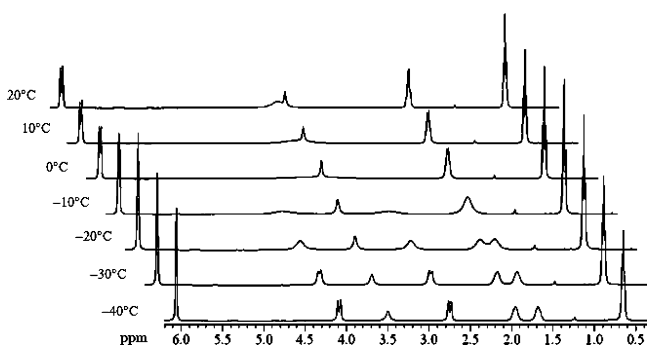
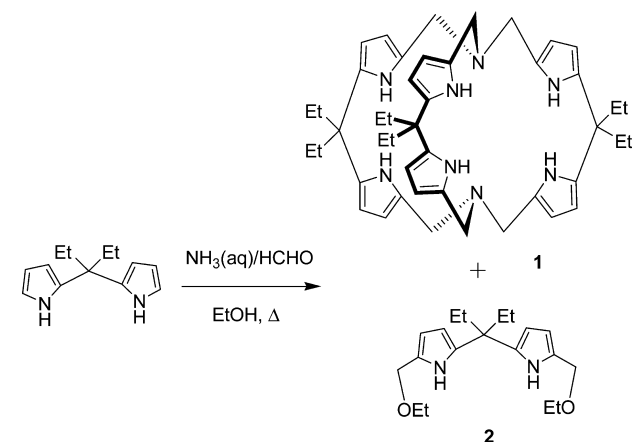
Scheme 1. Synthesis of Macrocyclic Azacryptand, **1**, and 1,9-Bis(ethoxymethyl)diethylpiperrolylmethane, **2**

Figure 1. Variable-temperature ^1H NMR spectra (400 MHz) of **1** in CDCl_3 (0.07 M). The peak at δ 3.5 ppm is due to water.

^{13}C NMR spectrum at -40°C has no change from the room temperature spectrum (see Supporting Information (SI)).

The observed broad resonance of $-\text{NCH}_2-$ protons at room temperature, which becomes a sharp singlet at 60°C (see SI), can be attributed to the fast interconversion between the staggered and the eclipsed conformations on the NMR time scale, caused by the torsional motion about the $\text{N}---\text{N}$ axis which can be through pyrrole ring flippings (Figure 2). These conformers

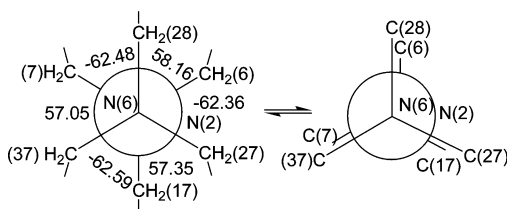


Figure 2. Newman projections about $\text{N}---\text{N}$ axis with dihedral angles (degrees) for **1**, as observed in its X-ray structure, showing the interconversion between the staggered and the eclipsed conformations in solution at room temperature. Atoms are labeled as in the crystal structure.

are observed in the solid state structures of **1** and **4** (*vide infra*), respectively. The low-temperature NMR pattern can be explained using a Newman projection along any one of the bridgehead nitrogen–carbon ($\text{N}-\text{C}$) bond axes as observed in the crystal structure of either **1** or **4** (see SI, Figure S15 and S16). When the temperature is lowered, the $\text{N}---\text{N}$ torsional

motion is slowed down and the energetically favorable staggered *in/in* conformation could have frozen, as supported by its crystal structure. As shown in the Newman projection (see SI, Figure S15), there are six diastereotopic $-\text{NCH}_2-$ methylene protons of the type H_A and H_B . Each bridgehead nitrogen side has three H_A and three H_B protons and each type giving one broad signal of equal intensity at lower temperatures that splits into a doublet due to the geminal coupling, $J = 13.2$ Hz, resulting in a resolved AB pattern at -40°C . Furthermore, an analogous AB pattern for the $-\text{NCH}_2-$ methylene protons (see SI, Figure S35) was observed in the ^1H NMR titration spectra of **1** with fluoride ion, showing the formation of the fluoride inclusion complex (*vide infra*). This frozen solid state staggered *in/in* conformer can also render diastereotopicity to the methylene protons of the *meso*-carbon ethyl groups, which appear as two broad resonances; the β -pyrrolic protons become equivalent and appear as a singlet. The Gibbs free energy of activation (ΔG_c^\ddagger) for the torsional motion of the pyrrole ring was calculated¹³ to be 54.5 kJ/mol using the parameters: $T_c = 293$ K, $\Delta\nu = 526$ Hz, and $k_c = 1168$ s⁻¹, which is in the range reported for other cryptands.^{8b,c}

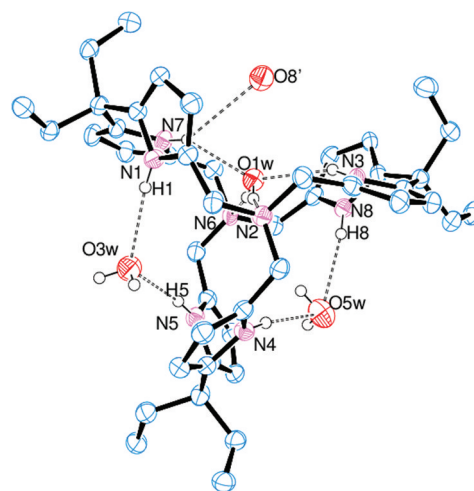


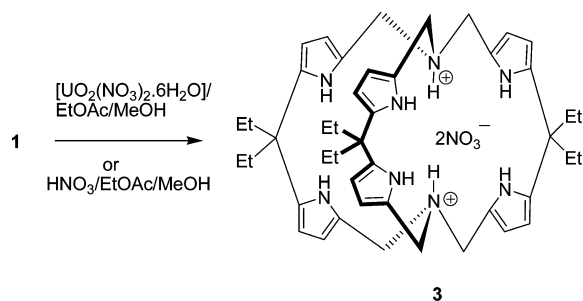
Figure 3. ORTEP diagram of $[\text{1}\cdot 4\text{H}_2\text{O}]_2$ with 30% probability ellipsoids. One of the two molecules present in the asymmetric unit is given. Most H atoms are omitted for clarity. Selected bond lengths (\AA) and angles (degrees): $\text{N}(7)\cdots\text{O}(1\text{W})$ 2.972(4), $\text{N}(7)-\text{H}(7)\cdots\text{O}(1\text{W})$ 142.6; $\text{O}(1\text{W})\cdots\text{N}(6)$ 2.903(4), $\text{O}(1\text{W})-\text{HIW1}\cdots\text{N}(6)$ 160.2; $\text{O}(1\text{W})\cdots\text{N}(2)$ 2.889(4), $\text{O}(1\text{W})-\text{H2W1}\cdots\text{N}(2)$ 154.4.

The structure of **1** was confirmed by X-ray (Figure 3), which is supported by its (+)ESI-MS spectrum. The compound crystallizes in the centrosymmetric $Pbca$ space group with two molecules in the asymmetric unit $[\text{1}\cdot 4\text{H}_2\text{O}]_2$, which are bridged via the H-bonds from one of the eight water molecules in the structure (see SI). Each molecule has an approximate C_3 symmetry along the vector passing through the bridgehead nitrogens and has different $\text{N}---\text{N}$ distances: 5.639 and 5.434 \AA . Both molecules have an *in/in* configuration as shown by the pyramidal geometry adopted by their nitrogen atoms, which are involved in H-bond interactions with the encapsulated water molecule in the cavity. In addition, the pyrrolic NH protons of each wing are directed opposite to each other and form H-bonds with the three water molecules located in the clefts and with the encapsulated water molecule.

The byproduct **2** formed in the Mannich reaction of dipyrrolylmethane was also characterized by both spectroscopic and X-ray methods. Details of the structure are given in SI.

Anion Coordination and Binding Studies. To investigate anion coordination chemistry of the azacryptand **1**, the nitrate complex **3** was synthesized in 91% yield by the reaction between **1** and one equivalent of $\text{UO}_2(\text{NO}_3)_2 \cdot 6\text{H}_2\text{O}$ in EtOAc/MeOH or THF/water mixture (Scheme 2). The analogous

Scheme 2. Synthesis of the Nitrate Anion Complex **3**



reaction of **1** with metal nitrates such as $\text{Al}(\text{NO}_3)_3 \cdot 9\text{H}_2\text{O}$ or $\text{Fe}(\text{NO}_3)_3 \cdot 9\text{H}_2\text{O}$, in which the metal has a greater charge-to-size ratio, in THF/water mixture also gave **3**. On the contrary, **3** was not formed when **1** was treated with NaNO_3 alone, but formed in the presence of HCl, indicating the requirement of a proton source. Thus the reaction between **1** and two equivalents of HNO_3 in EtOAc/MeOH mixture afforded the nitrate complex **3** in 88% crystalline yield. The formation of **3** from the highly Lewis acidic metal centers can be through the hydrolysis reactions.¹⁴

The ^1H NMR spectrum of **3** features two broad multiplets at δ 3.60 and δ 4.97 for the $-\text{NCH}_2-$ methylene protons due to their coupling with the ammonium hydrogens (N^+H), indicating asymmetric nitrate ion interactions. The presence of the nitrate anion was confirmed by its IR stretching frequency at 1384 cm^{-1} .

The X-ray structure of $[\text{H}_2\mathbf{1}]^{2+}[\text{NO}_3^-]_2 \cdot 5\text{H}_2\text{O}$, **3** (Figure 4) revealed a staggered conformation about the N---N axis and two nitrate anions asymmetrically bound one each to two of its three clefts via both H-bonds and electrostatic interactions from the two ammonium cations formed by protonation of the bridgehead nitrogen atoms.¹⁵ In the structure, both ammonium hydrogen atoms are pointing toward the cavity and are H-bonded to the encapsulated water molecule. The two pyrrolic NH protons of each dipyrrolylmethane subunit are directed opposite to each other and form H-bonds, including bifurcated, with the disordered nitrate anions. In addition to the three water molecules located in the crystal lattice, the oxygen atom of the water molecule located in the third cleft is chelated by the pyrrolic NH protons. Each nitrate ion has three different N---O bond distances owing to its asymmetric binding. For example, N(10)---O(9) bond distance (1.279 Å), whose O atom has three H-bonds, is longer than other two N---O distances (1.233 and 1.224 Å), whose O atoms have two and none H-bonds, respectively. This is probably because of decrease of π -electron density in the N---O bonds, when H-bonded.¹⁶ It is interesting to note that the nitrate anion is unable to replace the water molecule present inside the cavity in **1**, indicating the lack of size and geometrical complementarity of the nitrate anion for encapsulation. The distance between the two bridgehead nitrogen atoms is increased to

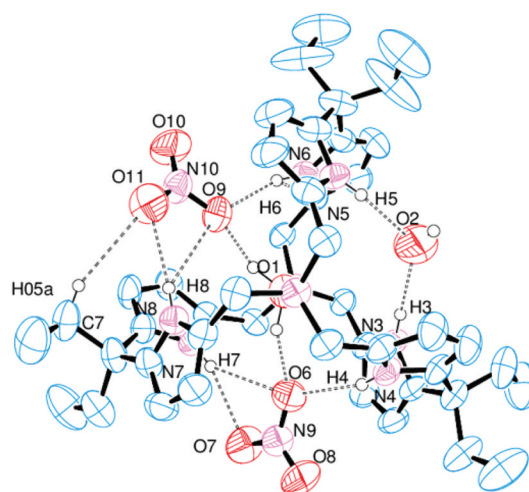


Figure 4. ORTEP diagram of $[\text{H}_2\mathbf{1}]^{2+}[\text{NO}_3^-]_2 \cdot 5\text{H}_2\text{O}$, **3** with 30% probability ellipsoids. Most H atoms and three water molecules are omitted for clarity. Selected bond lengths (Å) and angles (degrees): N(10)---O(10) 1.224(6), N(10)---O(9) 1.278(6), N(10)---O(11) 1.233(6), N(4)---O(6) 2.898(7), N(4)---H(4)---O(6) 160(4); N(7)---O(6) 3.400(7), N(7)---H(7)---O(6) 149(4); N(7)---O(7) 3.103(7), N(7)---H(7)---O(7) 160(4); N(6)---O(9) 2.853(7), N(6)---H(6)---O(9) 165(4); N(8)---O(11) 3.059(8), N(8)---H(8)---O(11) 166(4); N(8)---O(9), 3.450(8), N(8)---H(8)---O(9) 141(4).

5.826 Å as compared to those in **1**, owing to the interactions of the nitrate anions.

The anion binding studies of **1** were carried out by ^1H NMR titrations. The NH resonance of the receptor was followed and the binding constants K_a were determined by EQNMR with a model of 1:1 (host/guest).¹⁷ The fitted binding isotherms and binding constants are given in Figure 8 and Table 1, respectively.

Table 1. Binding Constants Determined by ^1H NMR Titrations for **1** with Anions as their $n\text{-Bu}_4\text{N}^+$ Salts in Acetone- d_6 at 298 K

	F^-	Cl^-	Br^-	NO_3^-	HSO_4^-	H_2PO_4^-
$\Delta\delta^a$ (ppm)	3.30 ^b	1.27	0.55	0.53	0.39	0.31
K_a (M^{-1})	$>10^4$, ^b	422 ^c	51 ^c	26 ^c	64 ^d	103 ^d

^a $\Delta\delta$ = the difference in the pyrrolic NH proton chemical shift between the free receptor and the anion complexed receptor from EQNMR calculation. ^bSlow complexation equilibrium and K_a was calculated by the method given in ref 17b (see SI), though the fluoride-mediated proton-deuterium exchange is going on. ^c<10% error. ^d<15% error.

The ^1H NMR titration spectra of **1** with fluoride ion in acetone- d_6 showed a slow complexation equilibrium and the pyrrolic NH resonance appeared as a doublet with a coupling constant, $J(\text{HF}) = 29.6\text{ Hz}$ (Figure 5), indicating a strong interaction and encapsulation of fluoride ion in the cavity of the neutral receptor **1**. For confirming the fluoride ion inclusion in the cavity and to monitor the proton-deuterium exchanges, the proton coupled ^{19}F NMR spectra of **1** (Figure 6) were recorded at different mole ratios of F^- . The spectrum recorded immediately after the addition of 0.5 equiv of F^- in acetone- d_6 showed six broad singlets (Figure 6b), without showing $J(\text{HF})$ coupling that is observed in the ^1H NMR spectrum, at δ -51.4, -51.8, -52.3, -52.8, -53.2, -53.7, exhibiting 0.4 or 0.5 ppm chemical shift difference between any two adjacent signals. These singlets can be tentatively assigned to the fluoride complex **4** and its deuterium exchanged forms represented by

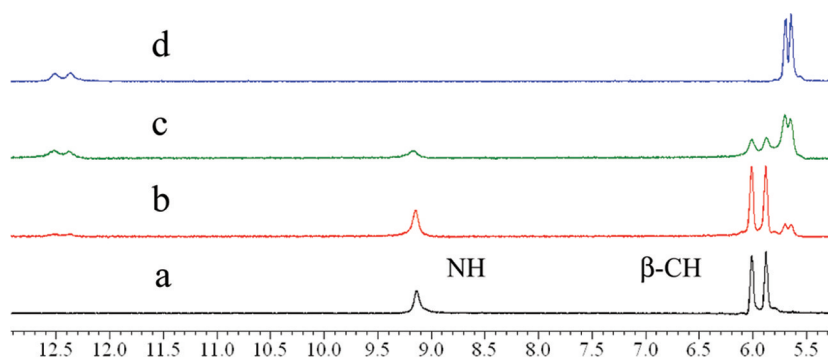


Figure 5. Partial ^1H NMR (200 MHz) spectra of (a) **1** (0.008 M) upon addition of (b) 0.2, (c) 0.6 and (d) 1 equiv of $n\text{-Bu}_4\text{NF}$ in acetone- d_6 at 298 K, showing the NH resonance splitting by fluoride ion and the slow complexation equilibrium.

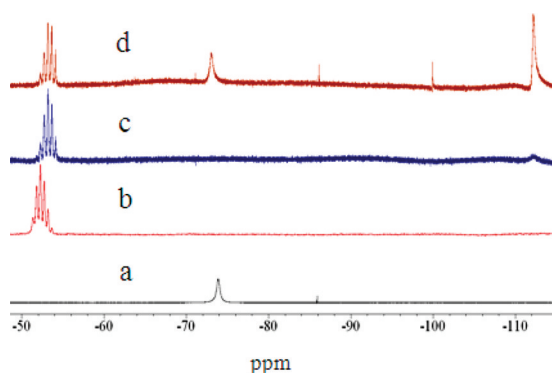


Figure 6. Proton coupled ^{19}F NMR (470.6 MHz) spectra of **1** (0.008 M) in acetone- d_6 at 298 K in the presence of different mole ratios of F^- : (a) $n\text{-Bu}_4\text{NF}$ in acetone- d_6 , (b) $[\mathbf{1}]:[n\text{-Bu}_4\text{NF}] = 1:0.5$, (c) $[\mathbf{1}]:[n\text{-Bu}_4\text{NF}] = 1:1$, and (d) $[\mathbf{1}]:[n\text{-Bu}_4\text{NF}] = 1:2$.

$\text{F}(\text{H}_3\text{D})$, $\text{F}(\text{H}_4\text{D}_2)$, $\text{F}(\text{H}_3\text{D}_3)$, $\text{F}(\text{H}_2\text{D}_4)$ and $\text{F}(\text{HD}_5)$, respectively, in which the pyrrolic NH protons are replaced by deuterium. Upon increasing the mole ratio of F^- to 1 equiv, the signal at $\delta -51.4$ (4) is disappeared and the new signals at $\delta -54.1$ and -112.2 are appeared (Figure 6c), which are again tentatively assigned to the fully deuterium exchanged complex $\text{F}(\text{D}_6)$ and HF_2^- , respectively. Further addition of F^- (two equiv) caused the signal at $\delta -51.8$ ($\text{F}(\text{H}_3\text{D})$) to disappear, but the other signal positions remained the same (Figure 6d). In addition, this spectrum also showed the signals of increased intensity for the free fluoride ion and HF_2^- . This indicates the deuterium exchange process is fast in the presence of more amount of F^- , leading to the formation of more amounts of the deuterium exchanged fluoride complexes and concomitant formation of HF_2^- . Furthermore, while the ^1H NMR spectrum of **1** with two equiv of F^- in acetone- d_6 was not showing a triplet for HF_2^- , the same composition in DMSO- d_6 showed a triplet at $\delta 16.11$ with $J(\text{HF}) = 122.5$ Hz in the ^1H NMR spectrum (Figure 7), probably because of a slow proton–deuterium exchange as demonstrated by Bowman-James,¹⁸ Jurczak¹⁹ and co-workers. Conversely, here the fluoride-mediated deuterium exchanges of the receptor **1** with acetone- d_6 can be fast enough at room temperature so that the $J(\text{HF})$ coupling is not seen in the fluorine NMR spectrum²⁰ but is observed in the ^1H spectrum.²¹

As can be seen from Table 1, the receptor **1** in its neutral form binds with F^- with $K_a > 10^4 \text{ M}^{-1}$, which is the largest value among the competitive anions studied. The greater binding constant K_a value is attributed to the combined effect

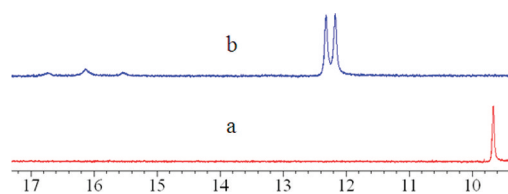


Figure 7. Partial ^1H NMR (200 MHz) spectra of (a) azacryptand **1** (0.008 M) in the presence of (b) 2 equiv of $n\text{-Bu}_4\text{NF}$ in DMSO- d_6 at 298 K, showing the formation of HF_2^- and the pyrrolic NH splitting.

of the specific size of the cavity into which F^- fits snugly due to its smaller size, the cooperative H-bonds from all pyrrolic NHs which causes a favorable conformational change for the receptor (see below) and the tendency of a fluoride ion to form a strong H-bond interaction. On the contrary, the binding constants for the larger size anions such as Cl^- , Br^- , NO_3^- , HSO_4^- and H_2PO_4^- are small and decrease as the size increases (from Cl^- to NO_3^-) (Table 1), which can be due to the unsuitable sizes and the cleft-bindings leading to weak interactions resulting from a limited potential hydrogen bond donors available in any one of the clefts in the neutral azacryptand molecules **1**, as compared to the interactions that an anion enjoys when encapsulated like fluoride ion. This is evidently shown by the crystal structure of the nitrate complex **3** in which the nitrate anions are bound to the clefts that offer only two pyrrolic NHs for hydrogen bondings (Figure 8).

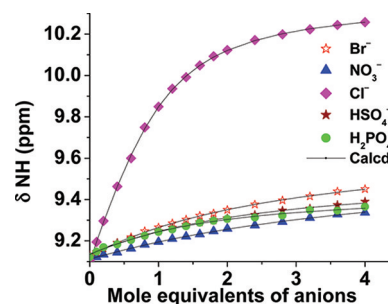


Figure 8. ^1H NMR (200 MHz) titration curve fittings for **1** (~ 0.008 M) with anions as their $n\text{-Bu}_4\text{N}^+$ salts in acetone- d_6 at 298 K.

The high selectivity of **1** toward fluoride ion was further confirmed by ^1H NMR. Addition of 1 equiv of F^- to a mixture of Cl^- , Br^- , NO_3^- , HSO_4^- , and H_2PO_4^- (1 equiv each) as their $n\text{-Bu}_4\text{N}^+$ salts in acetone- d_6 containing the receptor made the NH resonance shifted immediately to 12.43 ppm (F^- complex value)

from 9.97 ppm (close to the Cl^- complex value) and appeared as a doublet with the same $J(\text{HF})$ coupling constant observed before, indicating the affinity and the selectivity of the receptor for fluoride ion (see SI).

To support the solution state fluoride ion recognition event (Scheme 3), the structure of the fluoride ion inclusion complex $[\mathbf{1}\cdot\text{F}^-][n\text{-Bu}_4\text{N}^+]$, **4** was confirmed by X-ray (Figure 9), which

Scheme 3. Formation of the Fluoride Ion Inclusion Complex 4 in Acetone- d_6

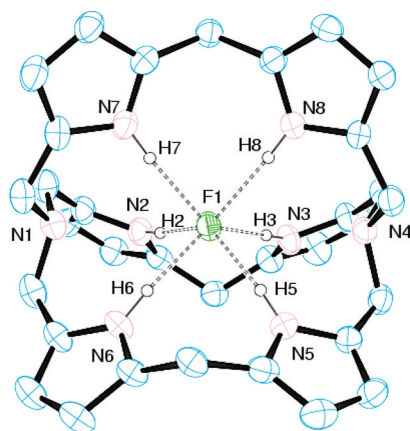
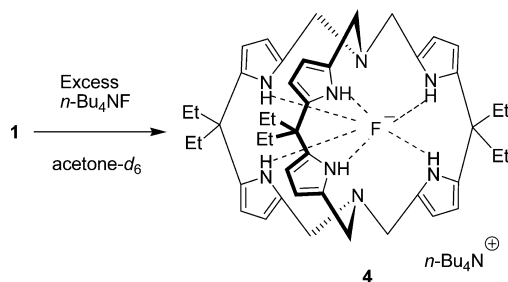


Figure 9. ORTEP diagram of $[\mathbf{1}\cdot\text{F}^-][n\text{-Bu}_4\text{N}^+]$, **4** with 30% probability ellipsoids. Most H atoms, *meso* ethyl groups and $n\text{-Bu}_4\text{N}^+$ group are omitted for clarity. Selected bond lengths (Å) and angles (degrees): N(2)⋯F(1) 2.860(4), N(2)–H(2)⋯F(1) 175(4); N(3)⋯F(1) 2.878(4), N(3)–H(3)⋯F(1) 176(4); N(5)⋯F(1) 2.859(4), N(5)–H(5)⋯F(1) 169(3); N(6)⋯F(1) 2.914(4), N(6)–H(6)⋯F(1) 165(3); N(7)⋯F(1) 2.867(4), N(7)–H(7)⋯F(1) 174(4); N(8)⋯F(1) 2.889(4), N(8)–H(8)⋯F(1) 172(3).

is supported by the (–)ESI-MS spectrum showing a peak m/z at 731.4915 (calcd mass 731.4925) corresponding to the mass of its $[\text{M}-n\text{-Bu}_4\text{N}^+]^-$ ion. The crystal structure revealed the encapsulation of the fluoride anion inside the cavity and all the pyrrolic NHs are involved in H-bond interactions giving a distorted trigonal prismatic geometry around F^- . The N⋯F distances range from 2.859(4) to 2.914(4) Å, which are longer than that (2.790(2) Å) reported for the monomacrocyclic calix[4]pyrrole fluoride complex,^{9p} but are shorter than the values (2.9457(18) to 3.1130(18) Å) reported for a polyamide cryptand fluoride complex.¹⁸ Although the neutral azacryptand molecule in **4** retains its *in/in* configuration, the complexation induces a change in the conformation, that is, the bridgehead N–C bonds are eclipsed and the structure has one 3-fold axis passing through both the bridgehead nitrogen and fluorine atoms, giving approximate C_{3h} symmetry. The distance between the bridgehead nitrogen atoms is enlarged to 6.446 Å, differing

by 0.807 and 1.012 Å as compared to values of **1**, which minimizes steric repulsions between the groups in the observed eclipsed conformation resulting from the torsional motion about N–N axis and the inclusion of fluoride ion in the cavity. A similar property has been reported for cryptands when forming cation inclusion complexes.²²

CONCLUSIONS

In conclusion, a new macrobicyclic azacryptand containing dipyrrolylmethane subunits with nitrogen bridgeheads and its fluoride inclusion and nitrate anion complexes were synthesized and structurally characterized. Interestingly, the azacryptand transforms from the staggered to eclipsed conformation to accommodate a fluoride ion in its cavity and this dynamic property was studied by variable-temperature NMR. Usually cryptands have a greater degree of selectivity than do monomacrocyclic analogs for a specific cation.^{23,2} Similarly, our cryptand-like molecule **1** as a neutral receptor has high affinity and selectivity toward fluoride ion over other anions studied in acetone, as compared to its monomacrocyclic containing dipyrrolylmethane subunits.^{12b} To the best of our knowledge, the conformational study and the structure of the fluoride cryptate **4** are the first examples among the known cryptand-like calixpyrrole systems.¹⁰

EXPERIMENTAL SECTION

Diethyldipyrrolylmethane was prepared by the literature procedure.²⁴ ^{19}F NMR spectra were recorded on 500 MHz spectrometer operating at 470.6 MHz and 0.05% trifluorotoluene in CDCl_3 was used as an external reference resonating at -62.74 ppm.

Synthesis of Azacryptand 1 and 2. *Method 1.* To a solution of freshly prepared diethyldipyrrolylmethane (2.5 g, 12.3 mmol) in ethanol (300 mL) was added aqueous NH_3 (25%, 0.56 mL, 8.2 mmol) at room temperature. Subsequently aqueous formaldehyde (39%, 1.9 mL, 24.7 mmol) was added and the solution was set to reflux at 70–80 °C for 1 day. After every 24 h, aqueous NH_3 (25%, 0.56 mL, 8.2 mmol) and aqueous formaldehyde (39%, 1.9 mL, 24.7 mmol) were added for three days and the solution was refluxed for five days in total. The color of the solution changed to reddish brown. The solvent was removed and the resultant residue was loaded onto a column filled with basic alumina. Elution using petroleum ether/ethylacetate mixture (v/v 30:1) afforded $\mathbf{1}\cdot 4\text{H}_2\text{O}$ (0.095 g, 0.121 mmol, 3%, with respect to diethyldipyrrolylmethane) as a colorless crystalline powder after solvent removal. Elution using petroleum ether/ethylacetate mixture (v/v 15:1) afforded **2** (0.125 g, 0.393 mmol, 3% with respect to diethyldipyrrolylmethane) as a colorless crystalline powder after solvent removal.

For **1**: mp >200 °C. ^1H NMR (400 MHz, CDCl_3 , 25 °C, ppm): δ = 0.66 (t, 18H, $^3J(\text{H,H})$ = 7.2 Hz), 1.83 (q, 12H, $^3J(\text{H,H})$ = 7.2 Hz), 3.42 (br s, 12H), 6.03 (dd, 12H), 8.46 (br s, 6H). $^{13}\text{C}\{^1\text{H}\}$ NMR (51.3 MHz, CDCl_3 , 25 °C, ppm): δ = 9.00, 31.6, 44.6, 51.6, 106.5, 110.4, 126.2, 136.6. FT-IR (KBr, cm^{-1}): ν = 3535 (m), 3351 (s), 2967 (s), 2933 (s), 2880 (w), 2794 (s), 1629 (m), 1586 (w), 1496 (m), 1449 (m), 1403 (w), 1378 (m), 1358 (m), 1329 (m), 1281 (w), 1226 (m), 1190 (m), 1073 (s), 1042 (s), 994 (w), 967 (m), 938 (m), 885 (w), 848 (w), 781 (vs), 699 (w), 652 (w), 584 (w). HRMS (+ESI): calcd m/z for $[\text{M} + \text{H}^+]$ $\text{C}_{45}\text{H}_{61}\text{N}_8$: 713.5019, found: 713.5011.

For **2**: mp 147 °C. ^1H NMR (200 MHz, CDCl_3 , 25 °C, ppm): δ = 0.71 (t, 6H, $^3J(\text{H,H})$ = 7.4 Hz), 1.14 (t, 6H, $^3J(\text{H,H})$ = 7.0 Hz), 1.92 (q, 4H, $^3J(\text{H,H})$ = 7.4 Hz), 3.41 (q, 4H, $^3J(\text{H,H})$ = 7.0 Hz), 4.36 (s, 4H), 6.01 (m, 4H), 7.91 (br s, 2H). $^{13}\text{C}\{^1\text{H}\}$ NMR (51.3 MHz, CDCl_3 , 25 °C, ppm): δ = 8.5, 15.3, 29.6, 43.8, 64.9, 65.5, 106.0, 107.7, 128.0, 137.4. FT-IR (KBr, cm^{-1}): ν = 3269 (vs), 3094 (w), 2966 (s), 2935 (m), 2871 (m), 1653 (w), 1497 (w), 1443 (w), 1357 (m), 1327 (w), 1283 (m), 1239 (w), 1205 (m), 1159 (w), 1116 (w), 1071 (vs), 1002 (m), 985 (m), 840 (m), 794 (s). HRMS (+ESI): calcd m/z for $[\text{M} + \text{Na}^+]$ $\text{C}_{19}\text{H}_{30}\text{N}_2\text{O}_2\text{Na}$: 341.2205 found: 341.2220.

Table 2. Crystallographic Data for Compounds [1·4H₂O]₂, 3 and 4

	[1·4H ₂ O] ₂	[H ₂ 1] ²⁺ [NO ₃ ⁻] ₂ ·5H ₂ O, 3	[1·F ⁻][<i>n</i> -Bu ₄ N ⁺] 4
Empirical formula	C ₄₅ H ₆₈ N ₈ O ₄	C ₄₅ H ₇₂ N ₁₀ O ₁₁	C ₆₁ H ₉₆ FN ₉
Formula weight	785.07	929.13	974.47
Wavelength (Å)	1.54178	0.71073	0.71073
Temperature (K)	110(2)	293(2)	293(2)
Crystal system	Orthorhombic	Monoclinic	Monoclinic
Color and shape	Colorless, Prism	Colorless, Plate	Colorless, Prism
Space group	<i>Pbca</i>	<i>P2₁/c</i>	<i>P2₁/c</i>
<i>a</i> /Å	25.823(8)	15.256(3)	13.148(3)
<i>b</i> /Å	25.671(9)	25.707(5)	23.572(6)
<i>c</i> /Å	26.199(9)	13.471(3)	19.584(5)
α /degree	90.00	90.00	90.00
β /degree	90.00	91.867(6)	100.538(8)
γ /degree	90.00	90.00	90.00
Volume (Å ³)	17368(10)	5280.2(17)	5967(3)
<i>Z</i>	16	4	4
<i>D</i> _{calcd} g cm ⁻³	1.201	1.169	1.085
μ /mm ⁻¹	0.616	0.085	0.066
<i>F</i> (000)	6816	2000	2136
Crystal size/mm	0.10 × 0.10 × 0.01	0.38 × 0.26 × 0.11	0.19 × 0.18 × 0.10
θ range/degree	2.96–60.00	1.55–25.00	1.37–25.00
Limiting indices	–29 < = <i>h</i> < = 29, –28 < = <i>k</i> < = 26, –29 < = <i>l</i> < = 29	–16 < = <i>h</i> < = 18, –30 < = <i>k</i> < = 30, –15 < = <i>l</i> < = 15	–15 < = <i>h</i> < = 15, –28 < = <i>k</i> < = 28, –22 < = <i>l</i> < = 23
Total/unique no. of reflns.	142232/12705	61300/9179	71276/10509
<i>R</i> _{int}	0.2923	0.1314	0.1533
Data/restr./ params.	12705/0/1055	9179/59/642	10509/15/658
GOF(<i>F</i> ²)	1.034	1.006	0.994
<i>R</i> ₁ , <i>wR</i> ₂	0.0694, 0.1255	0.0950, 0.2265	0.0700, 0.1657
<i>R</i> indices (all data)			
<i>R</i> ₁ , <i>wR</i> ₂	0.1356, 0.1468	0.1845, 0.2858	0.1860, 0.2212
Largest different peak and hole (e Å ⁻³)	0.524 and –0.214	0.608 and –0.272	0.720 and –0.286

Method II for 1. To a mixture of ammonium chloride (0.35 g, 6.59 mmol) and formaldehyde (39%, 1.52 mL, 19.7 mmol) in a small amount of water (2 mL), a solution of freshly prepared diethyl-dipyrrolylmethane (2.0 g, 9.81 mmol) in ethanol (200 mL) was added dropwise at 0 °C with stirring. After stirring the solution for 15 h at room temperature, solid sodium hydroxide (0.27 g, 6.59 mmol) was added and stirred for another 0.5 h to give a clear solution with little precipitate. The solvent was removed under vacuum and the resultant residue was extracted with dichloromethane three times. The dichloromethane solution was dried over anhydrous MgSO₄ and filtered. The solvent was removed and the resultant residue was loaded onto a column filled with basic alumina. Elution using petroleum ether/ethylacetate mixture (v/v 30:1) afforded 1·4H₂O (0.052 g, 0.066 mmol, 2.0%) as a colorless crystalline powder after solvent removal.

Synthesis of the Nitrate Complex [H₂1]²⁺[NO₃⁻]₂·5H₂O, 3.
Method I. To a solution of azacryptand 1·4H₂O (0.03 g, 0.038 mmol) in ethylacetate (5 mL)/methanol (5 mL) mixture, solid UO₂(NO₃)₂·6H₂O (0.019 g, 0.038 mmol) was added. After stirring for 10 min at room temperature, the resultant yellow solution was allowed to stand for the slow evaporation in a test tube. Colorless crystals of [H₂1]²⁺[NO₃⁻]₂·5H₂O, 3 formed over a period of 4–5 days. The solution was filtered and the crystals were washed with petroleum ether and dried in air (0.032 g, 0.034 mmol, 91%). mp >200 °C. ¹H NMR (200 MHz, CDCl₃, 25 °C, ppm): δ = 0.59 (t, 18H, ³J(H,H) = 7.2 Hz), 1.91 (q, 12H), 3.60 (br t, 6H), 4.97 (m, 6H), 6.14 (s, 6H), 6.29 (s, 6H), 7.61 (br s, 2H), 10.77 (br s, 6H). Due to its very poor solubility in CDCl₃ or acetone-*d*₆ or DMSO-*d*₆, ¹³C NMR could not be recorded. FT-IR (KBr, cm⁻¹): ν = 3259 (s), 2967 (m), 2936 (w), 2874 (w), 1655 (w), 1637 (w), 1508(w), 1490 (w), 1384 (vs), 1330 (m), 1281(w), 1214 (w), 1192 (w), 1049 (w), 1009 (m), 985 (w), 880 (w), 783 (m), 696 (w). Anal. Calcd for C₄₅H₇₂N₁₀O₁₁: C, 58.17; H, 7.81; N, 15.08. Found: C, 57.45; H, 8.07; N, 14.77.

Method II. To a solution of azacryptand 1·4H₂O (0.05 g, 0.064 mmol) in ethylacetate (8 mL)/methanol (8 mL) mixture, concentrated nitric acid (16M, 7.95 μ L, 0.13 mmol) was added and mixed well. The solution was allowed to evaporate slowly. The color of the solution changed to deep reddish brown and colorless crystals of [H₂1]²⁺[NO₃⁻]₂·5H₂O, 3 formed over a period of 4–5 days (0.052 g, 0.056 mmol, 88%).

Method III. To a solution of azacryptand 1·4H₂O (0.025 g, 0.031 mmol) in THF (10 mL)/methanol (10 mL) mixture, a mixture of HCl (1.2 M, 53 μ L, 0.064 mmol) and NaNO₃ (0.054 g, 0.064 mmol) in water (2 mL) was added dropwise. After stirring for 5 min at room temperature, the solution was allowed to stand for the slow evaporation to give colorless plates of [H₂1]²⁺[NO₃⁻]₂·5H₂O, 3 over a period of 4–5 days (0.022 g, 0.024 mmol, 76%).

Method IV. To a solution of azacryptand 1·4H₂O (0.009 g, 0.011 mmol) in THF (8 mL)/water (2 mL) mixture, solid Fe(NO₃)₃·9H₂O (0.0046 g, 0.011 mmol) or Al(NO₃)₃·9H₂O (0.0043 g, 0.011 mmol) was added. After stirring for 10 min, the solution was filtered and the filtrate was allowed to evaporate slowly to give crystals of 3. The ¹H NMR of 3 obtained by this method is the same as that of 3 obtained from above methods.

NMR Titrations. Using 10 μ L Hamilton Gastight syringe, all the titrations were carried out by adding an incremental amount of anions (F⁻, Cl⁻, Br⁻, NO₃⁻, HSO₄⁻, and H₂PO₄⁻) (2 μ L, 1 × 10⁻³ mmol, 0.2 equivalent) as their *n*-tetrabutylammonium salts (0.5 M) in acetone-*d*₆ to a NMR tube containing the receptor 1·4H₂O (4 mg, 0.005 mmol) in acetone-*d*₆ (0.6 mL). After each addition, the spectrum was recorded and the NH resonance was monitored for calculating the association constants *K*_a by the EQNMR program and by the Hirose two-parameter methods (see SI). Titrations in DMSO-*d*₆ were not carried out as 1·4H₂O is sparingly soluble.

X-Ray Crystallography. Suitable single crystals of **1** and **2** were obtained from a mixture of dichloromethane/petroleum ether (v/v 20/1). For **3**, single crystals were obtained from ethylacetate/methanol (v/v 1/1) mixture upon the slow evaporation. Suitable single crystals of the fluoride complex, $[1 \cdot F^-][n\text{-Bu}_4N^+]$ **4** were obtained from acetone- d_6 solution containing the receptor **1** and $n\text{-Bu}_4NF$ (50 equiv) upon the slow evaporation.

Single crystal X-ray diffraction data collections for **2**, **3** and **4** were performed using Bruker-APEX-II CCD diffractometer with graphite monochromated $Mo_{K\alpha}$ radiation ($\lambda = 0.71073 \text{ \AA}$). For $[1 \cdot 4H_2O]$ **2**, the data collection was performed using MWPC area detector diffractometer with $Cu_{K\alpha}$ radiation ($\lambda = 1.54178 \text{ \AA}$) at 110 K. The structures were solved by direct methods, which successfully located most of the non-hydrogen atoms. Subsequently, least-squares refinements were carried out on F^2 using SHELXL-97 (WinGX version)²⁵ to locate the remaining non-hydrogen atoms. All non-hydrogen atoms were refined anisotropically and the hydrogen atoms were refined isotropically on calculated positions using a riding model except the pyrrolic NH and the ammonium hydrogen atoms in the structures **2**, **3** and **4**, which were located from the difference Fourier map and refined isotropically with restraints SADI and with the thermal parameters equivalent to 1.2 times the value of the nitrogen atom to which the hydrogen atom is bonded. In the structure of $[1 \cdot 4H_2O]$ **2**, two water molecule oxygen atoms (O6 and O8) are disordered and their hydrogen atoms are not fixed. In the case of $[H_2I]^{2+}[NO_3^-]_2 \cdot 5H_2O$ **3**, two of the ethyl groups, C37–C38 and C39–C40, are disordered over two positions with the site occupancy factors of 64% and 36%. The nitrate anion (N9) is disordered over two positions with the site occupancy factors of 86% and 14%; the other nitrate anion (N10) is also disordered over two positions with the site occupancy factors of 78% and 22%. These were handled with EADP and SADI options available in the SHELXL-97 program. Other perspective views of the structures and packing diagrams are given in the Supporting Information. Crystallographic refinement data are given in Table 2.

■ ASSOCIATED CONTENT

■ Supporting Information

NMR, IR, crystallographic data (CIF), perspective views of X-ray structures and details of binding constants calculations. This material is available free of charge via the Internet at <http://pubs.acs.org>.

■ AUTHOR INFORMATION

■ Corresponding Author

*gmani@chem.iitkgp.ernet.in

■ ACKNOWLEDGMENTS

We thank the CSIR and DST for support and for the X-ray and NMR facilities. We also thank Dr. Carola Schulzke, Trinity College, Dublin for HRMS, Dr. Joseph H. Reibenspies, Department of Chemistry, Texas A&M University for a data collection and structure refinements and Dr. Swadhin Mandal, Indian Institute of Science Education and Research, Kolkata for ^{19}F NMR spectra.

■ REFERENCES

- (1) Park, C. H.; Simmons, H. E. *J. Am. Chem. Soc.* **1968**, *90*, 2431–2432.
- (2) Dietrich, B.; Viout, P.; Lehn, J.-M. *Macrocyclic Chemistry*; VCH Verlagsgesellschaft mbH: Weinheim, Germany, 1993.
- (3) (a) Bianchi, A.; Bowman-James, K.; García-España, E. *Supramolecular Chemistry of Anions*; Wiley-VCH: New York, 1997. (b) Sessler, J. L.; Gale, P. A.; Cho, W.-S. *Anion Receptor Chemistry*; Royal Society of Chemistry: Cambridge, 2006.

(4) For reviews, see: (a) Cametti, M.; Rissanen, K. *Chem. Commun.* **2009**, 2809–2829. (b) Wade, C. R.; Broomsgrove, A. E. J.; Aldridge, S.; Gabbai, F. P. *Chem. Rev.* **2010**, *110*, 3958–3984.

(5) For reviews, see: (a) Beer, P. D.; Gale, P. A. *Angew. Chem., Int. Ed.* **2001**, *40*, 486–516. (b) McKee, V.; Nelson, J.; Town, R. M. *Chem. Soc. Rev.* **2003**, *32*, 309–325. (c) Choi, K.; Hamilton, A. D. *Coord. Chem. Rev.* **2003**, *240*, 101–110. (d) Filby, M. H.; Steed, J. W. *Coord. Chem. Rev.* **2006**, *250*, 3200–3218. (e) Joyce, L. A.; Shabbir, S. H.; Ansllyn, E. V. *Chem. Soc. Rev.* **2010**, *39*, 3621–3632. (f) Dydio, P.; Lichosyt, D.; Jurczak, J. *Chem. Soc. Rev.* **2011**, *40*, 2971–2985. For articles, for example, see: (g) Mendy, J. S.; Pilate, M. L.; Horne, T.; Day, V. W.; Hossain, M. A. *Chem. Commun.* **2010**, *46*, 6084–6086. (h) Ziach, K.; Ceborska, M.; Jurczak, J. *Tetrahedron Lett.* **2011**, *52*, 4452–4455, and references therein.

(6) Kang, S. O.; Llinares, J. M.; Day, V. W.; Bowman-James, K. *Chem. Soc. Rev.* **2010**, *39*, 3980–4003.

(7) (a) Reilly, S. D.; Khalsa, G. R. K.; Ford, D. K.; Brainard, J. R.; Hay, B. P.; Smith, P. H. *Inorg. Chem.* **1995**, *34*, 569–575. (b) Dietrich, B.; Dilworth, B.; Lehn, J.-M.; Souchez, J.-P.; Cesario, M.; Guilhem, J.; Pascard, C. *Helv. Chim. Acta* **1996**, *79*, 569–587.

(8) (a) Dietrich, B.; Lehn, J. M.; Sauvage, J. P.; Blanzat, J. *Tetrahedron* **1973**, *29*, 1629–1645. (b) Kunze, A.; Bethke, S.; Gleiter, R.; Rominger, F. *Org. Lett.* **2000**, *2*, 609–612. (c) Bonnot, C.; Chambron, J.-C.; Espinosa, E.; Graff, R. *J. Org. Chem.* **2008**, *73*, 868–881.

(9) (a) Kee, S.-Y.; Lim, J. M.; Kim, S.-J.; Yoo, J.; Park, J.-S.; Sarma, T.; Lynch, V. M.; Panda, P. K.; Sessler, J. L.; Kim, D.; Lee, C.-H. *Chem. Commun.* **2011**, *47*, 6813–6815. (b) Rambo, B. M.; Sessler, J. L. *Chem.–Eur. J.* **2011**, *17*, 4946–4959. (c) Fisher, M. G.; Gale, P. A.; Hiscock, J. R.; Hursthouse, M. B.; Light, M. E.; Schmidtchen, F. P.; Tong, C. C. *Chem. Commun.* **2009**, 3017–3019. (d) Dehaen, W.; Gale, P. A.; García-Garrido, S. E.; Kostermans, M.; Light, M. E. *New J. Chem.* **2007**, *31*, 691–696. (e) Lee, C.-H.; Lee, J.-S.; Na, H.-K.; Yoon, D.-W.; Miyaji, H.; Cho, W.-S.; Sessler, J. L. *J. Org. Chem.* **2005**, *70*, 2067–2074. (f) Sessler, J. L.; An, D.; Cho, W. S.; Lynch, V. *Angew. Chem., Int. Ed.* **2003**, *42*, 2278–2281. (g) Cafeo, G.; Kohnke, F. H.; Parisi, M. F.; Nascone, R. P.; La Torre, G. L.; Williams, D. J. *Org. Lett.* **2002**, *4*, 2695–2697. (h) Turner, B.; Shterenberg, A.; Kapon, M.; Botoshansky, M.; Suwinska, K.; Eichen, Y. *Chem. Commun.* **2002**, 726–727. (i) Cafeo, G.; Kohnke, F. H.; La Torre, G. L.; Parisi, M. F.; Nascone, R. P.; White, A. J. P.; Williams, D. J. *Chem.–Eur. J.* **2002**, *8*, 3148–3156. (j) Turner, B.; Shterenberg, A.; Kapon, M.; Suwinska, K.; Eichen, Y. *Chem. Commun.* **2001**, 13–14. (k) Cafeo, G.; Kohnke, F. H.; La Torre, G. L.; White, A. J. P.; Williams, D. J. *Angew. Chem., Int. Ed.* **2000**, *39*, 1496–1498. (l) Cafeo, G.; Kohnke, F. H.; La Torre, G. L.; White, A. J. P.; Williams, D. J. *Chem. Commun.* **2000**, 1207–1208. (m) Sessler, J. L.; Anzenbacher, P. Jr.; Shriver, J. A.; Jursíková, K.; Lynch, V. M.; Marquez, M. J. *Am. Chem. Soc.* **2000**, *122*, 12061–12062. (n) Depraetere, S.; Smet, M.; Dehaen, W. *Angew. Chem., Int. Ed.* **1999**, *38*, 3359–3361. (o) Turner, B.; Botoshansky, M.; Eichen, Y. *Angew. Chem., Int. Ed.* **1998**, *37*, 2475–2478. (p) Gale, P. A.; Sessler, J. L.; Král, V.; Lynch, V. *J. Am. Chem. Soc.* **1996**, *118*, 5140–5141.

(10) (a) Bucher, C.; Zimmerman, R. S.; Lynch, V.; Sessler, J. L. *J. Am. Chem. Soc.* **2001**, *123*, 9716–9717. (b) Bucher, C.; Zimmerman, R. S.; Lynch, V.; Sessler, J. L. *Chem. Commun.* **2003**, 1646–1647. (c) Beer, P. D.; Cheetham, A. G.; Drew, M. G. B.; Fox, O. D.; Hayes, E. J.; Rolls, T. D. *Dalton Trans.* **2003**, 603–611. (d) Fox, O. D.; Rolls, T. D.; Drew, M. G. B.; Beer, P. D. *Chem. Commun.* **2001**, 1632–1633. (e) Cafeo, G.; Colquhoun, H. M.; Cuzzola, A.; Gattuso, M.; Kohnke, F. H.; Valenti, L.; White, A. J. P. *J. Org. Chem.* **2010**, *75*, 6263–6266.

(11) (a) Haynes, C. J. E.; Gale, P. A. *Chem. Commun.* **2011**, *47*, 8203–8209. (b) Gale, P. A. *Acc. Chem. Res.* **2011**, *44*, 216–226.

(12) (a) Mani, G.; Jana, D.; Kumar, R.; Ghorai, D. *Org. Lett.* **2010**, *12*, 3212–3215. (b) Mani, G.; Guchhait, T.; Kumar, R.; Kumar, S. *Org. Lett.* **2010**, *12*, 3910–3913.

(13) (a) The free energy of activation was calculated using the simplified equation given in reference 8c: $\Delta G^\ddagger = 2.303RT_c(10.319 + \log T_c - \log k_c)$ kJ/mol; $k_c = \pi\Delta\nu/\sqrt{2} \text{ s}^{-1}$. (b) Fischer, P.; Fetting, A. *Magn. Reson. Chem.* **1997**, *35*, 839–844.

(14) Huheey, J. E.; Keiter, E. A.; Keiter, R. L.; Medhi, O. K. *Inorganic Chemistry*; Dorling Kindersley (India) Pvt. Ltd., Pearson Education: New Delhi, 2007; p 225.

(15) Cleft bindings of nitrate ion by other macrobicycles are known. For example, see: (a) Saeed, M. A.; Fronczek, F. R.; Huang, M. -J.; Hossain, M. A. *Chem. Commun.* **2010**, 46, 404–406. (b) Clifford, T.; Danby, A.; Llinares, J. M.; Mason, S.; Alcock, N. W.; Powell, D.; Aguilar, J. A.; Garica-España, E.; Bowman-James, K. *Inorg. Chem.* **2001**, 40, 4710–4720. (c) Bisson, A. P.; Lynch, V. M.; Monahan, M. -K. C.; Anslyn, E. V. *Angew. Chem., Int. Ed.* **1997**, 36, 2340–2342.

(16) (a) Mahoney, J. M.; Stucker, K. A.; Jiang, H.; Carmichael, I.; Brinkmann, N. R.; Beatty, A. M.; Noll, B. C.; Smith, B. D. *J. Am. Chem. Soc.* **2005**, 127, 2922–2928. (b) Hay, B. P.; Gutowski, M.; Dixon, D. A.; Garza, J.; Vargas, R.; Moyer, B. A. *J. Am. Chem. Soc.* **2004**, 126, 7925–7934.

(17) (a) Hynes, M. J. *J. Chem. Soc., Dalton Trans.* **1993**, 311–312. (b) Hirose, K. *J. Inclusion Phenom. Macrocyclic Chem.* **2001**, 39, 193–209.

(18) Kang, S. O.; VanderVelde, D.; Powell, D.; Bowman-James, K. *J. Am. Chem. Soc.* **2004**, 126, 12272–12273.

(19) Chmielewski, M. J.; Jurczak, J. *Chem.–Eur. J.* **2005**, 11, 6080–6094.

(20) (a) Libra, E. R.; Scott, M. J. *Chem. Commun.* **2006**, 1485–1487. (b) Kang, S. O.; Day, V. W.; Bowman-James, K. *Inorg. Chem.* **2010**, 49, 8629–8636. (c) Shionoya, M.; Furuta, H.; Lynch, V.; Harriman, A.; Sessler, J. L. *J. Am. Chem. Soc.* **1992**, 114, 5714–5722.

(21) (a) Kang, S. O.; Day, V. W.; Bowman-James, K. *J. Org. Chem.* **2010**, 75, 277–283. (b) Nishiyabu, R.; Anzenbacher, P. Jr. *Org. Lett.* **2006**, 8, 359–362. (c) Camiolo, S.; Gale, P. A. *Chem. Commun.* **2000**, 1129–1130. (d) Gale, P. A.; Sessler, J. L.; Král, V. *Chem. Commun.* **1998**, 1–8.

(22) Metz, B.; Moras, D.; Weiss, R. *J. Chem. Soc., Chem. Commun.* **1971**, 444–445.

(23) Steed, J. W.; Atwood, J. L. *Supramolecular Chemistry*; Wiley: Chichester, 2009.

(24) Sobral, A. J. F. N.; Rebanda, N. G. C. L.; Silva, M. D.; Lampreia, S. H.; Silva, M. R.; Beja, A. M.; Paixao, J. A.; Gonsalves, A. M. A. R. *Tetrahedron Lett.* **2003**, 44, 3971–3973.

(25) Sheldrick, G. M. A short history of SHELX. *Acta Crystallogr.* **2008**, A64, 112–122.